Laser spectroscopy of the 1001-nm ground-state transition in dysprosium

D. Studer, L. Maske, P. Windpassinger, and K. Wendt
Institut für Physik, Johannes Gutenberg-Universität Mainz, 55128 Mainz, Germany

(Received 20 July 2018; published 10 October 2018)

We present a direct excitation of the presumably ultranarrow 1001-nm ground-state transition in atomic dysprosium. By using resonance ionization spectroscopy with pulsed Ti:sapphire lasers at a hot cavity laser ion source, we were able to measure the isotopic shifts in the 1001-nm line between all seven stable isotopes. Furthermore, we determined the upper level energy from the atomic transition frequency of the ^{164}Dy isotope as 9991.004(1) cm^{-1} and confirm the level energy listed in the NIST database. Since a sufficiently narrow natural linewidth is an essential prerequisite for high-precision spectroscopic investigations for fundamental questions, we furthermore determined a lower limit of 2.9(1) μs for the lifetime of the excited state.

DOI: 10.1103/PhysRevA.98.042504

I. INTRODUCTION

Narrow-linewidth atomic transitions can serve as highly sensitive probes for various inner and outer atomic interaction potentials and respective forces, and have become a general-purpose tool in the field of quantum many-body physics [1,2]. In addition, narrow linewidth is usually accompanied with long lifetimes of the excited states, such that these transitions offer precise, coherent control over metastable state populations and therefore allow for, e.g., the study of quantum gas mixtures and Kondo-type physics [3,4] or the implementation of qubits [5,6]. Beyond that, precision isotope shift measurements [7] have been suggested as a vehicle to reveal high-energy physics contributions to atomic spectra and search for physics beyond the standard model [8–10]. Various atomic species possess ultranarrow transitions; however, dysprosium is a particularly interesting case. Because of its high magnetic moment and consequent anisotropic long-range interaction, dysprosium is highly attractive for quantum many-body physics. On the other hand, many high-energy effects scale with atomic mass. Thus, dysprosium, with about 160 nucleons and seven stable isotopes, is an ideal study case. Finding and characterizing a particularly narrow optical transitions in this system therefore is of high relevance.

Some promising narrow-linewidth transitions are discussed in Ref. [11], including calculated level energies and lifetimes which are compared to experimental values, if available. One is the 1001-nm $4f^{10}6s^2(^5I_8) \rightarrow 4f^9(^6H^o)5d6s^2(^7I^o_9)$ ground-state transition with a theoretically predicted linewidth of 53 Hz [11]. It was first observed indirectly in the spectrum of an induction lamp filled with ^{162}Dy [12]. The NIST database [13] reports an energy of 9990.97(1) cm^{-1} for the upper level, which corresponds to a transition wavelength of 1000.904(1) nm. In contrast, calculations using the configuration interaction (CI) method yield a value of 9944 cm^{-1} (corresponding to 1005.6 nm) [11]. This and the fact that the transition at 1001 nm could not be detected via fluorescence laser spectroscopy in an atomic beam [14] motivate the verification of either result.

In order to detect this weak transition, we use the highly efficient technique of laser resonance ionization spectroscopy (RIS) [15]. The aims of this work are to (i) determine the exact transition frequency and extract first values for the isotope shifts of all stable isotopes and (ii) give a lower limit for the lifetime of the excited state, since a sufficiently narrow natural linewidth is a prerequisite for precision spectroscopy.

II. EXPERIMENTAL

A. Setup

Laser resonance ionization is based on multistep photoionization via characteristic transitions of the element under investigation. Because of the typically high efficiency and selectivity, this technique is often applied at radioactive ion beam facilities, such as ISOLDE at CERN, both for ion beam production [16,17] and spectroscopy of short-lived radioisotopes [18–20].

Similarly, our setup is optimized with respect to high sensitivity and relies on the hot-cavity laser ion source technique, combined with a low-energy quadrupole mass spectrometer. Figure 1 shows a sketch of the apparatus. A detailed description is given in Ref. [21]. In our experiment, we use a sample of $\approx 10^{15}$ Dy atoms, prepared from a standard nitric acid solution,[1] which is enclosed in a 3×3 mm^2 Zr carrier foil and introduced into a tantalum oven 35 mm long with an inner diameter of 2 mm. Dysprosium atoms are ionized by three properly synchronized laser pulses at a repetition rate of 10 kHz. The laser beams are overlapped anticollinearly with the ion beam axis, so that ionization takes place directly inside the atomizer oven. Alternatively, one may guide the laser beams through a side window of the vacuum chamber, perpendicularly intersecting the effusing atomic beam in front of the oven. This significantly reduces spectral Doppler broadening at the cost of approximately two orders of magnitude in ionization efficiency.

[1]Alfa Aesar Dysprosium AAS.

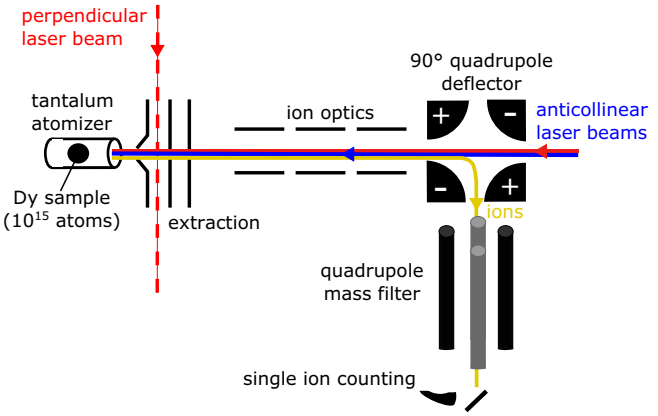

FIG. 1. Sketch of the atomic beam mass spectrometer with ion flight path (yellow) and laser beams in anticollinear (solid red, solid blue) and perpendicular, crossed beam (dashed red) geometry. In the latter case, the first extraction electrode is put on a positive voltage to act as an ion repeller.

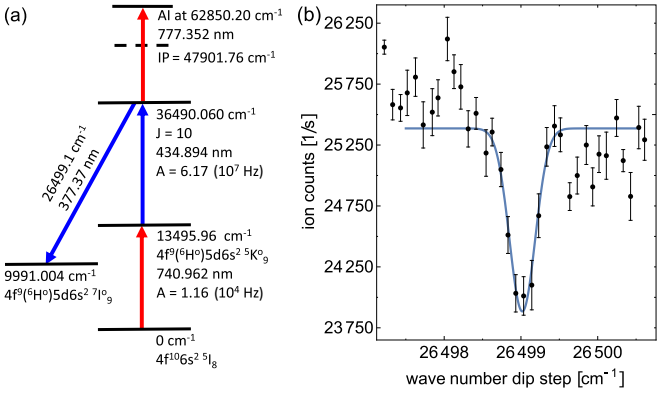

FIG. 2. Indirect measurement of the upper energy level belonging to the 1001-nm transition. (a) Measurement scheme consisting of a three-step resonant excitation, addressing an autoionizing state (AI) above the first ionization potential IP = 47901.76 cm^{-1} of dysprosium [28], together with the additional dip step. (b) Ion counts as a function of the dip-step wave number.

The laser system consists of up to four pulsed Ti:sapphire lasers, each of them pumped with 12 to 18 W of average power of a commercial 532-nm pulsed Nd:YAG laser.[2] The Ti:sapphire lasers have pulse lengths of typically 50 ns with up to 4 W average output power. They can be tuned from about 680 to 940 nm and have a spectral linewidth of 1–10 GHz depending on the specific resonator components used. The tuning range can be extended with second, third, and fourth harmonic generation. Details of the laser system are given in Refs. [22–24]. For wide-range scans, we use a modified laser design, featuring a diffraction grating in Littrow configuration for frequency selection [25]. This laser type has an output power of up to 2 W and can be tuned mode-hop-free from 700 to 1020 nm. Under optimal conditions the linewidth is 1.5 GHz; however, at wavelengths far from the Ti:sapphire gain maximum the pump power and the Ti:sapphire crystal position in the resonator have to be adjusted specifically so that the linewidth increases to 5 GHz. The fundamental output of each laser is measured with a wavelength meter.[3]

B. Spectroscopic technique

Spectroscopy is performed by detuning one laser in the excitation scheme while monitoring the ion count rate. Since this requires a photoionization scheme to begin with, the initial measurements were carried out with a scheme based on the $4f^{10}6s^2(^5I_8) \rightarrow 4f^9(^6H^o)5d\,6s^2(^5K_9^o)$ ground-state transition at 741 nm. The excited state has a configuration similar to the one at 1001 nm, but the line intensity is a factor of ≈50 higher [11,26]. This enormously facilitates the development of a full resonant three-step ionization scheme. Starting from the excited state of the 741-nm transition, a wide range spectrum of high-lying states was accessed by scanning the second harmonics of a grating-assisted Ti:sapphire laser between 401 and 437 nm. A third laser at 780 nm (the gain maximum of Ti:sapphire) is used for nonresonant ionization of excited atoms. The spectrum shows over 100 lines, with some of the upper states known in literature [13]. A complete list of recorded lines is given in the Supplementary Material [27]. In most cases, a resonant third excitation step to an autoionizing state can be easily found in the dense spectrum of dysprosium by detuning the ionization laser output by few nanometers.

To connect our photoionization scheme to the 1001-nm transition, we use a fourth laser to de-excite atoms from the second excited state into the $4f^9(^6H^o)5d\,6s^2(^7I_9^o)$ state. When the laser is resonant to the transition, the de-excitation competes with the ionization and a dip in the ion signal can be observed, as shown in Fig. 2.

The rather weak dip signal of less than 10% of the total ion counts may be related to the fact that the specifically induced de-excitation competes with a number of loss channels through spontaneous decay into other lower lying levels. With the dip technique, we cannot only indirectly measure the level energy of the excited state but also prepare for a full-resonant three-step ionization scheme for the direct excitation of the 1001-nm ground-state transition. To further reduce the uncertainty of the $4f^9(^6H^o)5d\,6s^2(^7I_9^o)$ level energy, which depends on three wavelengths in the dip measurements, we proceed by using the settled ionization scheme involving the direct excitation of the 1001-nm transition.

III. DIRECT EXCITATION SPECTROSCOPY

A. The 1001-nm transition

In this section, we discuss a direct excitation of the 1001-nm ground-state transition. For the measurements, all laser beams are oriented anticollinearly to the atom beam (see Fig. 1). A perpendicular geometry does not lead to an improvement at this point, since the expected Doppler broadening of ≈600 MHz within the tantalum oven is in the order of the laser linewidth. The beam diameter at atom position is about 2 mm which corresponds to the inner diameter of the oven. For the photoionization a Ti:sapphire laser with

[2]Photonics Industries DM100-532.

[3]High Finesse WS6-600 for wide-range scans and High Finesse WSU-30 for isotope shift measurements.

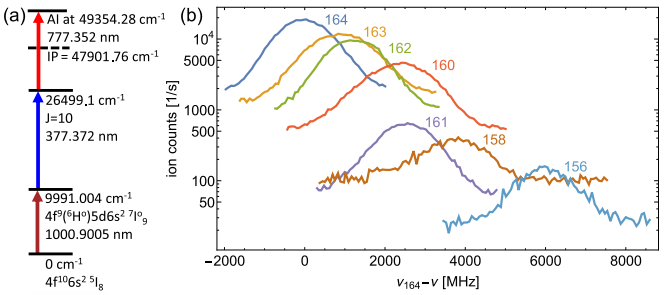

FIG. 3. Isotope shift measurement for the 1001-nm ground-state transition. (a) Excitation scheme. (b) Ion counts as a function of first excitation step frequency ν relative to the atomic transition frequency $\nu_{164} = 299.5228(1)$ THz of the ^{164}Dy isotope.

a wavelength of 1001 nm first excites the atoms into the $4f^9(^6H^o)5d\,6s^2(^7I^o_9)$ state. From this state, the atoms are resonantly excited to the second excited state with an energy of 26499.1 cm^{-1} with a wavelength of 377 nm by using a second, this time frequency-doubled, Ti:sapphire laser. In the last step, a third laser with a wavelength of 777 nm addresses an autoionizing state to resonantly ionize the atoms. The complete excitation scheme is shown in Fig. 3(a).

While the frequencies of the upper two steps are fixed for the whole measurement, the frequency of the first step is scanned. Because of its wide tuning range, the grating assisted laser, as described in Sec. II A, was used to probe the 1001-nm transition, while an additional etalon ($d = 2$ mm, $R = 0.4$) was inserted to reduce the linewidth to 1 GHz. Figure 3(b) shows the resulting direct excitation of all seven stable dysprosium isotopes. For the individual isotopes, we adapted the mass spectrometer setting accordingly.

From the measurement, we calculated the isotopic shifts in the 1001-nm transition, which are listed in Table I.

The specified error corresponds to the sum of the fit error and an estimated error of 30 MHz for the drift of the wavelength meter during the measuring time. Any other systematics are comparatively small and were neglected. The error estimation is based on later measurements in which we determined the drift as ≈10 MHz per hour as well as the long measuring time due to the individual mass spectrometer setting for each isotope. Furthermore, we determined the upper level energy from the atomic transition frequency of the ^{164}Dy isotope as 9991.004(1) cm^{-1}. Taking the isotope shift into account, the latter is in good agreement with the value listed in the NIST database [13].

TABLE I. Isotope shift in the 1001-nm transition in Dy, relative to the isotope 164.

	Isotope shift $\delta\nu$ [MHz]
$\delta\nu_{164-163}$	907(36)
$\delta\nu_{164-162}$	1233(35)
$\delta\nu_{164-161}$	2337(37)
$\delta\nu_{164-160}$	2566(36)
$\delta\nu_{164-158}$	3685(45)
$\delta\nu_{164-156}$	5976(39)

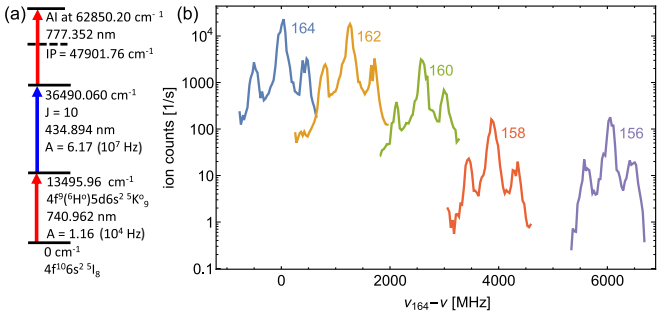

FIG. 4. Isotope shift measurement for the 741-nm ground-state transition. (a) Excitation scheme. (b) Ion counts as a function of first excitation step frequency ν relative to the atomic transition frequency $\nu_{164} = 404.5990(1)$ THz of the ^{164}Dy isotope. Laser side modes are clearly visible.

B. The 741-nm transition

In the course of the indirect detection of the upper energy level belonging to the 1001-nm transition, we were also able to measure the isotope shift in the first excitation step along the 741-nm ground-state transition. These data were measured with a different implementation of the standard Ti:sapphire laser featuring a bow-tie resonator design. Similar to the standard laser, frequency selection is achieved by a combination of a birefringent filter and a solid etalon ($d = 0.3$ mm, $R = 0.4$), but with the option to add an additional piezo-actuated air-spaced etalon ($d = 12$ mm, $R = 0.4$). This potentially allows operation on a single longitudinal mode; however, since the cavity lacks active stabilization at this stage, it suffers from an occasional rise of side modes, which appear at $\delta\nu = \pm 443$ MHz and are suppressed by only about a factor of ≈10.

Figure 4 shows the direct excitation of the five stable bosonic isotopes and Table II shows the resulting isotope shifts. Since the isotope shifts of the stable odd-mass isotopes with nonzero nuclear spin I as well as the isotope shifts of the three stable even-mass isotopes ($I = 0$) with highest abundance are already given in Ref. [26], we omitted a re-measurement of the odd-mass isotopes at this point. The isotope shifts obtained here for the even-mass isotopes with highest abundance are in accordance with Ref. [26]. However, here we have also provided an isotope shift measurement in this line for the two rarest stable isotopes, ^{158}Dy and ^{156}Dy.

IV. LIFETIME MEASUREMENTS

Lower limits for the lifetimes of the excited states at 9990.96 and 13495.96 cm^{-1} can be determined by

TABLE II. Isotope shift in the 741-nm transition in Dy for the five isotopes with even mass number.

	Isotope shift $\delta\nu$ [MHz]
$\delta\nu_{164-162}$	1245(32)
$\delta\nu_{164-160}$	2583(32)
$\delta\nu_{164-158}$	3874(32)
$\delta\nu_{164-156}$	6042(32)

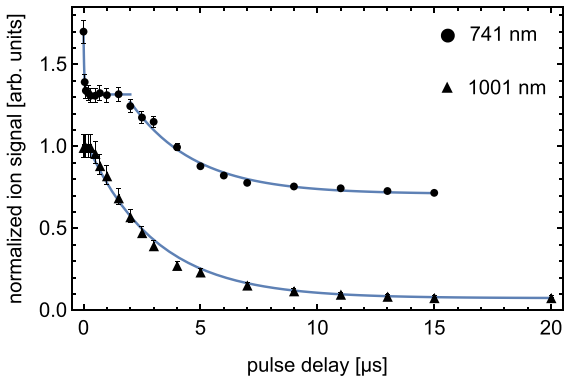

FIG. 5. Lifetime measurements in the 741- and 1001-nm transitions obtained by delaying the ionization laser pulse. For better readability, we added a random offset to the ion signal of the 741-nm transition.

investigating the population decay after the pulsed laser excitation. The population is probed by delayed ionization laser pulses, according to the excitation schemes in Secs. III A and III B, and subsequent ion counting. The temporal profiles and delays between the individual Ti:sapphire laser pulses are captured by fast photodiodes and monitored with an oscilloscope. In order to maintain stable laser power during the measurement, the first excitation step laser is pumped by a separate Nd:YAG laser[4] and pulse delays are controlled by means of shifting the pump laser trigger accordingly. Figure 5 shows the excited-state population decay at oven temperatures of 700(100) °C and 950(100) °C for the states at 9990.96 and 13495.96 cm^{-1}, respectively. The excited state at 9990.96 cm^{-1} shows an exponential decay with a lifetime of 2.9(1) μs, whereas the 13495.96 cm^{-1} state clearly features two components with lifetimes of 32(2) ns and 2.8(3) μs. The short-lived contribution is an artifact, which is related to the ionization scheme for the 741-nm transition where the first excitation step has enough energy to ionize atoms parasitically from the second excited state. This effect is completely suppressed by a delayed second excitation pulse; thus, the 32(2)-ns lifetime corresponds to the laser pulse length. Nonetheless, lifetimes of the investigated states are orders of magnitude shorter than theoretical values [11], which actually was expected due to the experimental circumstances. De-excitation of atoms within the hot atomic vapor may occur by collisions with the oven wall or other atoms. In comparison to an experimental value for the lifetime of the 13495.96 cm^{-1} excited state of 89.3(8) μs [26] and the fact that both of our measured values agree with each other we can conclude that, in our experiment, the extracted lifetimes predominantly depend on the mean free path of the hot atoms within the atomic beam oven cavity. Consequently, the 2.9(1) μs lifetime for the 9990.96 cm^{-1} excited state should be treated as a very conservative lower limit, which corresponds to an upper limit for the 1001-nm transition linewidth of 55(2) kHz.

[4]Quantronix Hawk-Pro 532-60-M.

V. CONCLUSION

We presented a direct excitation of the 1001-nm ground-state transition for all seven stable dysprosium isotopes for the first time by applying high-repetition-rate pulsed laser resonance ionization. Furthermore, we measured the isotopic shift in the 1001-nm transition and determined the upper level energy from the atomic transition frequency of the ^{164}Dy isotope as 9991.004(1) cm^{-1}, which is in accordance with the value listed in the NIST database [13]. We obtain an upper limit of 55(2) kHz for the transition linewidth of the excited state. Our results open the route toward investigation of physics beyond the standard model of particle physics and enable the study of many-body physics with magnetic quantum gases by atomic high-resolution spectroscopy within the 1001-nm transition.

ACKNOWLEDGMENTS

The authors would like to point out that this work is part of the M.Sc. thesis of L. Maske, who not only contributed to the experimental activities but also did a major part of the data evaluation. We thank N. Petersen and F. Mühlbauer for their ideas and fruitful discussions. We gratefully acknowledge the financial support of the EU through ENSAR2-RESIST (Grant No. 654002) and DFG Großgerät: DFG FUGG (INST 247/818-1).

[1] A. Yamaguchi, S. Uetake, S. Kato, H. Ito, and Y. Takahashi, New J. Phys. **12**, 103001 (2010).
[2] M. J. Martin, M. Bishof, M. D. Swallows, X. Zhang, C. Benko, J. von Stecher, A. V. Gorshkov, A. M. Rey, and J. Ye, Science **341**, 632 (2013).
[3] M. Foss-Feig, M. Hermele, and A. M. Rey, Phys. Rev. A **81**, 051603(R) (2010).
[4] L. Riegger, N. Darkwah Oppong, M. Höfer, D. R. Fernandes, I. Bloch, and S. Fölling, Phys. Rev. Lett. **120**, 143601 (2018).
[5] A. J. Daley, M. M. Boyd, J. Ye, and P. Zoller, Phys. Rev. Lett. **101**, 170504 (2008).
[6] A. V. Gorshkov, A. M. Rey, A. J. Daley, M. M. Boyd, J. Ye, P. Zoller, and M. D. Lukin, Phys. Rev. Lett. **102**, 110503 (2009).
[7] W. H. King, J. Opt. Soc. Am. **53**, 638 (1963).
[8] V. V. Flambaum, A. J. Geddes, and A. V. Viatkina, Phys. Rev. A **97**, 032510 (2018).
[9] J. C. Berengut, D. Budker, C. Delaunay, V. V. Flambaum, C. Frugiuele, E. Fuchs, C. Grojean, R. Harnik, R. Ozeri, G. Perez, and Y. Soreq, Phys. Rev. Lett. **120**, 091801 (2018).
[10] C. Delaunay, R. Ozeri, G. Perez, and Y. Soreq, Phys. Rev. D **96**, 093001 (2017).
[11] V. A. Dzuba and V. V. Flambaum, Phys. Rev. A **81**, 052515 (2010).
[12] J. G. Conway and E. F. Worden, J. Opt. Soc. Am. **61**, 704 (1971).

[13] A. Kramida, Y. Ralchenko, J. Reader, and the NIST ASD Team, NIST Atomic Spectra Database, https://www.nist.gov/pml/atomic-spectra-database.
[14] M. Lu, N. Q. Burdick, S. H. Youn, and B. L. Lev, Phys. Rev. Lett. **107**, 190401 (2011).
[15] V. S. Letokhov and V. I. Mishin, Opt. Commun. **29**, 168 (1979).
[16] V. N. Fedosseev, Y. Kudryavtsev, and V. I. Mishin, Phys. Scr. **85**, 058104 (2012).
[17] J. Lassen, P. Bricault, M. Dombsky, J. P. Lavoie, C. Geppert, and K. Wendt, Hyperfine Interact. **162**, 69 (2006).
[18] T. E. Cocolios, H. H. Al Suradi, J. Billowes, I. Budinčević, R. P. de Groote, S. de Schepper, V. N. Fedosseev, K. T. Flanagan, S. Franchoo, R. F. Garcia Ruiz *et al.*, Nucl. Instrum. Methods Phys. Res., Sect. B **317**, 565 (2013).
[19] S. Rothe, A. N. Andreyev, S. Antalic, A. Borschevsky, L. Capponi, T. E. Cocolios, H. de Witte, E. Eliav, D. V. Fedorov, V. N. Fedosseev *et al.*, Nat. Commun. **4**, 1835 (2013).
[20] R. P. de Groote, M. Verlinde, V. Sonnenschein, K. T. Flanagan, I. Moore, and G. Neyens, Phys. Rev. A **95**, 032502 (2017).
[21] V. Sonnenschein, S. Raeder, A. Hakimi, I. D. Moore, and K. Wendt, J. Phys. B: At., Mol. Opt. Phys. **45**, 165005 (2012).
[22] S. Rothe, B. A. Marsh, C. Mattolat, V. N. Fedosseev, and K. Wendt, J. Phys.: Conf. Ser. **312**, 052020 (2011).
[23] V. Sonnenschein, I. D. Moore, H. Khan, I. Pohjalainen, and M. Reponen, Hyperfine Interact. **227**, 113 (2014).
[24] S. Wolf, D. Studer, K. Wendt, and F. Schmidt-Kaler, Appl. Phys. B **124**, 412 (2018).
[25] A. Teigelhöfer, P. Bricault, O. Chachkova, M. Gillner, J. Lassen, J. P. Lavoie, R. Li, J. Meißner, W. Neu, and K. D. A. Wendt, Hyperfine Interact. **196**, 161 (2010).
[26] M. Lu, S. H. Youn, and B. L. Lev, Phys. Rev. A **83**, 012510 (2011).
[27] See Supplemental Material at http://link.aps.org/supplemental/10.1103/PhysRevA.98.042504 for list of atomic transitions starting from the 13495.96 cm^{-1} excited state.
[28] D. Studer, P. Dyrauf, P. Naubereit, R. Heinke, and K. Wendt, Hyperfine Interact. **238**, 02A916 (2017).